



A soft anionic hydrogel reactor for silver nanoparticle preparation and use in H₂ production, 4-nitrophenol reduction and alcohol oxidation

Massomeh Ghorbanloo¹ · Paeizeh Nazari¹

Published online: 10 August 2019

© Springer Science+Business Media, LLC, part of Springer Nature 2019

Abstract

Poly(2-acrylamido-2-methyl-1-propanesulfonic acid) (p(AMPS)) hydrogels were synthesized via free radical polymerization reaction technique under mild reaction conditions. The chemical structure of synthesized p(AMPS) anionic macroporous hydrogel was confirmed by Fourier transform infrared (FT-IR), scanning electron microscopy (SEM). Synthesized hydrogels were used as template for in situ metal nanoparticle preparation by using Ag(CH₃COO) in H₂O. Metal nanoparticles embedded p(AMPS)-Ag were visualized by TEM. The metal content of composites was estimated via atomic absorption spectroscopy (AAS). This metal-nanoparticle porous hydrogel composite was employed in the reduction of 4-nitrophenol and H₂ generation from hydrolysis of sodium borohydride (NaBH₄). The activation energies, enthalpy, and entropy for 4-NP reduction and NaBH₄ hydrolysis catalyzed by composite were determined. P(AMPS)-Ag composite was also used as catalyst in the aerobic oxidation of alcohols by emphasizing the effects of different parameters such as temperature, substituent effect, etc. Finally, the catalysts were easily recovered from the reaction media and it could be re-used for the other four runs without significant loss of activity.

Keywords p(AMPS)-Ag composites · H₂ production · Nitro compound reduction · Aerobic oxidation

1 Introduction

Due to a highly effective and large number of potential applications, metal nanoparticles have brought a great revolution in the field of material science. The high surface energy and large surface area to volume ratio enable the metal nanoparticles to be applicable in many areas such as sensors, electronic devices, catalysts in many related fields from chemistry, and physics to biotechnology, and material science due to their nanoscale optical, electrical and catalytic properties [1, 2]. The surface area of nanoparticles is specifically important in heterogeneous catalysts. The main issue that hinders pervasive use of metal nanoparticles as a catalyst is

their high tendency to aggregate since their catalytic activity decreases upon aggregation due to the reduction in their surface area [1]. Aggregation and other issues regarding metal nanoparticles can be solved using stabilizing materials such as surfactants, linear polymers, zeolites, silicates, alumina, and zirconia [3–8]. In the metal nanoparticles preparation, for instance, one of the most commonly employed methods is the adsorption of stabilization agents such as linear polymer or surfactants onto metal nanoparticles to provide steric stabilization. The one significant drawback with this method is the decrease of catalytic activities of the metal nanoparticle as a result of the addition of these new species to its surface, although new impurities are also generated. Therefore, there is a great need for versatile and smart support materials. Hydrogels as smart materials and as huge water containers that derived from versatile polymeric materials by crosslinked three-dimensional networks can be suitable candidates for preparation of different metal nanoparticle in situ [9]. One of the applications of the metal nanoparticle containing hydrogel–metal composites is to provide reaction flask for various chemical reactions [10, 11]. Among all hydrogel networks, the environmentally benign ones are

Electronic supplementary material The online version of this article (<https://doi.org/10.1007/s10934-019-00794-y>) contains supplementary material, which is available to authorized users.

✉ Massomeh Ghorbanloo
m_ghorbanloo@yahoo.com

¹ Department of Chemistry, Faculty of Science, University of Zanjan, 45371-38791 Zanjan, Iran

particularly important due to three main advantages. First, they act as a template in which metal nanoparticles are prepared inside the hydrogel in a way that no aggregation occurs. Second, they provide an adaptable milieu for catalysis of a variety of reactions. Here, the catalytic reactions are occurring within the boundaries of hydrogels; therefore, no dramatic changes in the conditions of reactors are required in industrial applications [12]. Third, nanocomposite hydrogels can effectively combine the unique properties of the inorganic and organic components to achieve a synergistic effect [13].

Alcohol oxidation is one of the pivotal functional group transformations in organic chemistry [14]. Generally, oxidation is performed using stoichiometric amount of transition metal oxidants or sulfides that produces a large number of undesirable products, being becomes intolerable in today's environmentally conscious world [15]. Thus, the development of environmentally friendly catalytic oxidation of alcohol with molecular oxygen at atmospheric pressure in green solvent is an important and urgent work [16–18]. Recently, aerobic alcohol oxidation employing heterogeneous noble metal nanocatalyst has gained a significant amount of interest since it avoids the use of toxic materials and a large amount of oxidizing reagents while no by-product other than water is produced. Of all the noble metal nanocatalysts such as Ag [19], Au [20, 21], Pd [19, 22, 23], Pt [24] and Rh [25], Ag containing nanocatalysts have been promising since they are not prone to leaching as a result of over oxidation, and partly due to their high efficiency.

The emerging demand of energy along with environmental concerns regarding extensive fossil fuels usage, have highlighted the necessity for alternative energy sources [26–28]. Due to the high gravimetric energy density, ideal combustion efficiency, zero-emission and non-toxicity, hydrogen has been considered as a promising energy carriers [29]. The chemical energy per unit mass of hydrogen is 142 MJ kg^{-1} that is almost three times greater than that of any other fuel. As an example the chemical energy per unit mass of hydrocarbons is only 47 MJ kg^{-1} [29]. Since water is the only side-product of the combustion of hydrogen, it can be an alternative fuel in internal combustion engines, which would significantly reduce the atmospheric pollution [30]. However, the technological barriers regarding the hydrogen storage and delivery as a result of its gaseous nature and low density at room temperature have restrained hydrogen's numerous applications [31, 32]. Hence, solid hydrogen storage materials exhibiting high capacity and safety have gained intense attention. Sodium borohydride (NaBH_4) is one of the well-known chemical compounds with potential application for the hydrogen storage, since it has high hydrogen content (10.8 wt%), high volumetric hydrogen density ($113 \text{ kg m}^{-3} \text{ H}_2$), low production costs, potentially safe operation, and high stability under ambient

conditions [31, 32]. Although hydrogen generation reaction upon NaBH_4 hydrolysis is considerably slow, the reaction is spontaneous at room temperature, and can be accelerated in the presence of suitable catalysts.

Wastewater mostly discharged from the industrial plants and metropolis introduces many toxics and persistent pollutants [33]. These pollutants cause severe health problems on human and ecosystems; consequently, these materials must be removed to improve water quality and the environment. Amongst these pollutants, mainly phenols and their derivatives are crucial contaminants in wastewater because of their high toxicity, carcinogenic nature, high oxygen demand, and low biodegradability [34]. 4-NP and 2-NP are the two phenol derivatives that are widely used in the production of insecticide, fungicide, and dyes. The direct exposure to these pollutants causes inflammation of eyes, skin, and respiratory tract. Also, the allergic response may occur in case of prolonged contact with skin [35]. Various technologies, such as biodegradation, adsorption, catalytic wet oxidation, and advanced oxidation processes have been conventionally used for the treatments of phenols [36]. In spite of the available biological methods that are widely performed for the treatment of wastewater, the low degradation rate is one of the major disadvantages of these organic species. Hence, the use of new, smart materials with high degradation rate to remove various contaminations is demanded, so, in this investigation, we prepared 3-D macro hydrogels composites from 2-Acrylamido-2-methyl-1-propansulfonic acid (AMPS) as p(AMPS)-Ag as an environmentally benign material.

In the present study, we report a facile and scalable route to prepare new designed, catalytically active metallic silver in situ grown on p(AMPS) hydrogels. The resultant p(AMPS)-Ag catalyst shows an excellent catalytic performance for the hydrogen generation from NaBH_4 hydrolysis, reduction of 4-NP and oxidation of alcohols. More interestingly, the p(AMPS)-Ag catalyst can be easily separated after catalytic reaction and readily recycled over four successive reaction cycles. Since the eco-friendly and inexpensive p(AMPS)-Ag is catalytically effective with superior recyclability.

2 Materials and methods

2.1 General considerations

2-Acrylamido-2-methyl-1-propansulfonic acid (AMPS, aqueous solution containing 50 wt % water) as monomer, *N,N'*-methylenebisacrylamide (MBA) as crosslinker (99%, Across), ammonium persulfate (APS) as initiators (99%, Sigma Aldrich) and *N,N,N',N'*-tetramethylmethylenediamine (TEMED) as accelerator (98% Across) were used in hydrogel preparation. $\text{Ag}(\text{CH}_3\text{COO})$ (Merck) was used as metal

ion source. Sodium borohydride (NaBH_4 , 98%, Merck) was used in the reduction of metal ions to prepare metal nanoparticles. FT-IR spectra were recorded in KBr disks with a Bruker FT-IR spectrophotometer. The exact amount of the silver in the composites was determined by AA spectroscopy. Morphology of swollen p(AMPS) hydrogel was investigated with scanning electron microscopy (SEM) via MIRA3 TESCAN FE SEM and an accelerating voltage of 10 keV. The sample was swollen and quickly frozen in liquid nitrogen. The hydrogel was freeze-dried at $-50\text{ }^\circ\text{C}$ for 3 days to preserve their porous structure without any collapse. After that, the dried samples were deposited onto an aluminum stub and sputter-coated with gold for 60 s to enhance conductivity. Transmission electron microscopy (TEM, PHILIPLS CM-30) was used to find out the size of metal nanoparticles inside the hydrogel nanocomposites. The swollen hydrogel was finely grounded with the help of a soft ball and the resulted hydrogel nanocomposite samples were dispersed in 1 mL of ethanol and dropped on collodion film coated copper grid for TEM analysis. The atomic absorption analysis was carried out using Varian spectra AA 220 equipment. The reduction of nitrophenol was determined using Pharmacia Biotech Ultrospec 4000 UV-Vis spectroscopy. The specific surface areas, pore volume and pore size measurements of p(AMPS) hydrogel were determined using a surface area and porosity measuring device (Belzorp Japan 926). Dried p(AMPS) particles were degassed to remove moisture and other contaminants at $80\text{ }^\circ\text{C}$ for 6 h prior to adsorption analysis using a Flow Prep 060 Degasser. The reaction products of oxidation were determined and analyzed using an HP Agilent 6890 gas chromatograph equipped with a HP-5 capillary column (phenyl methyl siloxane $30\text{ m} \times 320\text{ }\mu\text{m} \times 0.25\text{ }\mu\text{m}$).

2.2 Preparation of hydrogel p(AMPS)

Polymeric hydrogel was synthesized from AMPS via free radical polymerization reaction techniques in the mild reaction condition ($30\text{ }^\circ\text{C}$), as shown in Scheme 1 [2]. In the synthesis of p(AMPS) hydrogels, 5 mL AMPS aqueous solution containing 50 wt% water, 0.093 g MBA and $5\text{ }\mu\text{L}$ TEMED were mixed with 0.5 mL pure water and to

this solution a separately prepared APS solution of 0.028 g APS in 0.5 mL water was added and vortexed homogeneously. The mixture was placed into plastic straws ($\sim 4\text{ mm}$ in diameter), and these plastic straws were immersed in a $30\text{ }^\circ\text{C}$ water bath for 4 h to complete polymerization and crosslinking. Finally, the obtained 3-D hydrogels were cut in equal shapes, washed with approximately of 2000 mL of water for 24 h. The wash water replenished every 2 h to remove un-reacted species (monomer, crosslinker, accelerator and initiator). After the cleaning procedure, hydrogels were dried in an oven to a constant weight at $40\text{ }^\circ\text{C}$ and kept in sealed containers for further use.

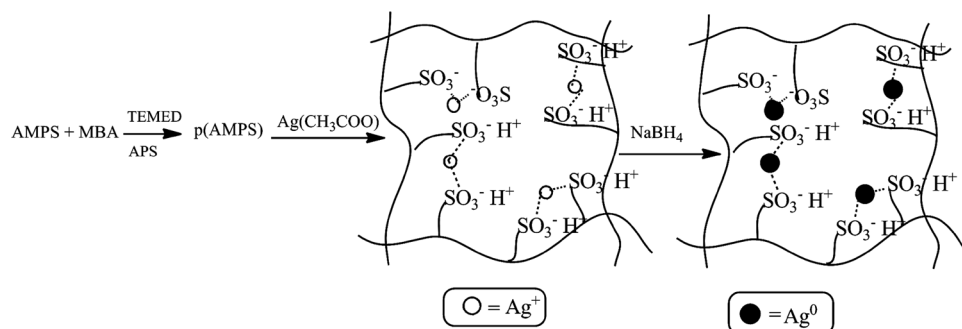
Selected FT-IR (KBr, cm^{-1}): (p(AMPS)): 3423 (br), 3114 (w), 3001 (w), 2950 (w), 1688 (m), 1568 (m), 1476 (w), 1404 (w), 1229 (s), 1053 (vs), 824 (w), 641 (w), 551 (w).

2.3 In situ synthesis of metal nanoparticles within p(AMPS) hydrogel

For in situ fabrication of metal nanoparticles within p(AMPS) hydrogel, first silver ions were loaded into hydrogel network by dispersing 0.2 g of the dried p(AMPS) hydrogel in 50 mL, 500 ppm aqueous solution of silver acetate for 24 h at room temperature under continuous stirring. Ag(I) ions loaded hydrogels were washed with DI to remove unbound metal ions. Then, to reduced metal ions within hydrogel network, metal ions loaded hydrogels were treated with 50 mL, 0.1 M NaBH_4 . Finally, the prepared p(AMPS)-Ag hydrogel composites were filtered, washed with DI and used for characterization, as shown in Scheme 1. The amounts of metal nanoparticles entrapped in hydrogels were calculated by AA measurements after dissolution of metal nanoparticles embedded within p(AMPS) hydrogel by treating with 5 M HNO_3 aqueous solution.

Selected FT-IR (KBr, cm^{-1}): (p(AMPS)-Ag): 3472 (br), 3028 (w), 2950 (w), 2880 (w), 1677 (m), 1563 (m), 1477 (w), 1412 (w), 1320 (w), 1231 (s), 1051 (s), 797 (w), 638 (w), 539 (w).

Scheme 1 Schematic representation for the synthesis of p(AMPS) composite



2.4 Swelling behavior of p(AMPS) hydrogel

The swelling experiments for the p(AMPS) hydrogel was carried out in water (at room temperature). Pre-weighted hydrogels were immersed in water and the mass increase was recorded by weighing the soaked hydrogels at certain time intervals after blot drying with filter paper to remove the excess solvent on the surface.

2.5 General reduction procedure

NaBH₄ (17.5 mmol) was added to solution of nitro compounds (0.5 mmol) in 50 mL of distilled water. Certain amount of dried hydrogel-composite was placed in this solution. After the addition catalysts (hydrogel composite), samples were directly withdrawn from the reaction medium at certain time intervals and diluted up to 15 times with DI followed by measuring UV–Vis spectra of these solutions to monitor the decrease in intensity of the absorption peak at 400 nm. The rate constant of the reaction was determined by measuring the change in intensity of this peak with time.

To study the effect of temperature on the rate of reduction of 4-NP, the reduction was carried out at three different temperatures; 25 °C, 40 °C and 60 °C keeping the amount of reactants and catalyst constant. Also the effect of amount of catalyst was investigated on the reduction of 4-NP. For this, different amounts of catalyst were used and other reaction conditions were kept constant. The reusability of the catalyst was also investigated by using the same catalyst in four consecutive runs in reduction reactions and p(AMPS)-Ag washed with DI water before each usage. All the experiments were repeated at least three times and their average values are given with standard deviations.

2.6 General oxidation procedure

A mixture of p(AMPS)-Ag in water (3.0 mL) was placed into a two-necked flask equipped with a magnetic stirrer. The flask was evacuated and refilled with pure oxygen (balloon filled). Then the benzyl alcohol (0.108 g, 1.0 mmol) was added into the solution with a syringe. The mixture was heated to reach the set temperature under O₂ atmosphere for 24 h. The resulting mixture was vigorously stirred at 80 °C under O₂ atmosphere for 24 h. After the reaction, the catalyst was de-swelled in CH₂Cl₂ (2.0 mL) for 24 h. Then the organic phase was combined and removed the solvent and analyzed immediately by GC. The oxidation products were identified by comparing the retention times with the literature data. For the blank test with the bare hydrogel without Ag, the oxidation reaction of benzyl alcohol was accomplished with p(AMPS). To test the reusability of the

p(AMPS)-Ag composite, after every usage, the catalyst was separated from reaction mixture by filtration, washed with DI and reused in the same reaction conditions again.

2.7 Hydrolysis of NaBH₄ catalyzed by p(AMPS)-Ag

In the hydrolysis of NaBH₄ certain amounts of hydrogel composites containing equal amounts of Ag nanoparticles were placed into 50 mL water at 25 °C. To initiate the hydrolysis reaction, 0.1 M (0.2 g) NaBH₄ was added to this reaction mixture and stirred at 1000 rpm. The volume of generated H₂ gas with time was measured in an experimental set up where the produced H₂ gas replaced water in an inverted volumetric cylinder. All the experiments were repeated at least three times and results are given as the averages of these three measurements with their standard deviations. To determine the effect of temperature on NaBH₄ hydrolysis and determine the activation parameters, 0.1 g p(AMPS)-Ag hydrogel composite was used in NaBH₄ hydrolysis at 25, 40 and 60 °C under the same reaction conditions.

3 Results and discussion

3.1 Synthesis and characterization

The characterization of porous p(AMPS) hydrogels and their metal composites were carried out with various characterization techniques, such as SEM images, FT-IR spectroscopy, TEM images and AA spectroscopy.

The structure of p(AMPS) hydrogels, were determined using a scanning electron microscope (SEM, JEOL 2010) on thin sections of freeze dried p(AMPS) hydrogels. The SEM image of p(AMPS), shown in Fig. 1, indicates the formation of homogeneous and highly porous material.

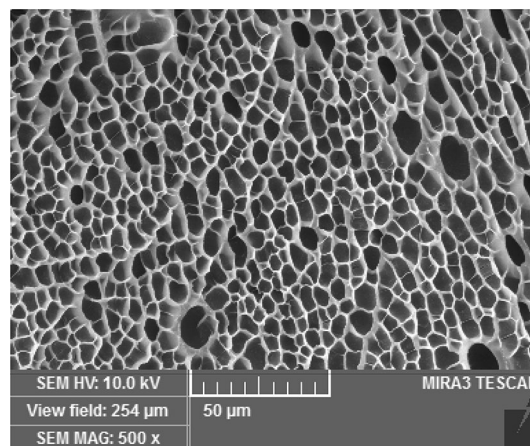


Fig. 1 SEM image of p(AMPS) hydrogel

To determine the swelling behavior of p(AMPS) hydrogels, distillation water was chosen as the swelling media. The swelling ratios were estimated using the following equation:

$$\text{Swelling ratio (\%)} = (W_s - W_d) / W_d \times 100$$

where, W_s is the weight of swollen hydrogel and W_d is the weight of the dried hydrogel at time zero. The swelling percent values of p(AMPS) hydrogel 740% in H_2O .

The representative FT-IR spectrum of p(AMPS) is shown in Fig. 2a. The main characteristic bands for AMPS shown at 3114 cm^{-1} , 2998 and 2950 cm^{-1} , 1688 cm^{-1} corresponds to N–H stretching, aliphatic -CH stretching, C=O stretching, respectively. The bands at 1229 cm^{-1} and 1058 cm^{-1} represent S–O stretching vibrations of sulfonic acid groups in AMPS units. As can be seen the bands the NH band of MBA is overlapped by OH band at about 3200 cm^{-1} [37], so the related peak is disordered.

In addition, porosity of p(AMPS) has been studied in dried solid state. Textural characterization of the p(AMPS) has been investigated using N_2 adsorption–desorption at $-196\text{ }^\circ\text{C}$. Figure 2 shows the pore size distribution of hydrogel obtained by Barrett–Joyner–Halendar (BJH) method. According to the isotherms of the sample, the specific surface area, specific pore volume and pore size distribution of the sample were obtained and the results are shown in Table 1. It can be seen that the pores are distributed in the region of mesoporous and macroporous. In the mesoporous region all samples exhibit a common peak between around 4 nm, indicating the presence of certain mesoporosity. On the other hand, all macoporous present a size below 100 nm.

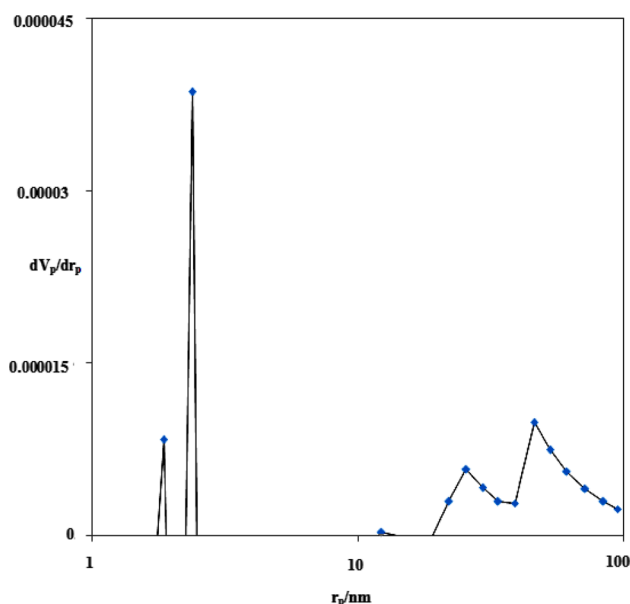


Fig. 2 Pore size distribution of p(AMPS) hydrogel

Table 1 Surface area and textural characteristics of samples

Sample	Specific surface area ($\text{m}^2\text{ g}^{-1}$)	Pore volume ($\text{cm}^3\text{ g}^{-1}$) ^a	Pore diameter (nm) ^b
P(AMPS)	0.325	0.0748	2.38

^a S_{BET} , calculated with the Brunauer–Emmett–Teller (BET) equation

^bDetermined by JBH method

A schematic representation of metal loading and in situ reduction process for the formation of metal nanoparticles inside hydrogel networks is demonstrated in Scheme 1. Firstly, the chemical changes in the structure of p(AMPS)-Ag composites were confirmed via FT-IR spectroscopy by recording the FT-IR spectra p(AMPS)-Ag as seen in Fig. 3b. After loading of Ag ions and reduction to Ag^0 nano-particles, the small shifts in FT-IR spectra of p(AMPS)-Ag is related to interactions between Ag and hydrogel matrix, as shown in Fig. 3b.

To investigate the nanostructure of the sample, TEM measurement was carried out. The TEM images of metal nanoparticles-containing p(AMPS) hydrogels are given in Fig. 4. As can be seen, metal nanoparticles with a uniform spherical shape, are distributed within p(AMPS) hydrogel matrices. Also p(AMPS)-Ag has about 20 nm, Fig. 5.

The amount of metal ion within the hydrogels was determined, by using AAS after dissolution by HNO_3 treatment and its amount is 4.3855 mmol/g hydrogel.

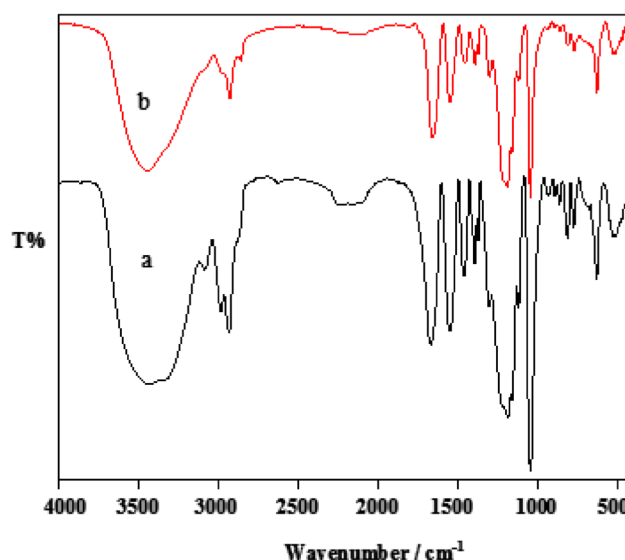


Fig. 3 FT-IR spectra of (a) p(AMPS) hydrogel, (b) p(AMPS)-Ag composite

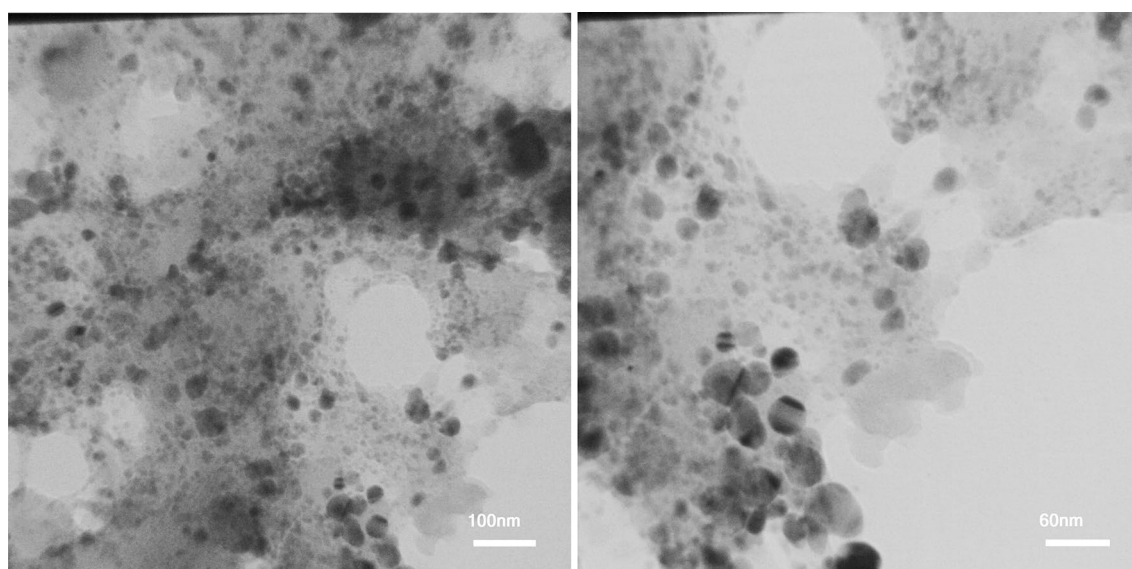


Fig. 4 TEM images of metal nanoparticles from p(AMPS)-Ag

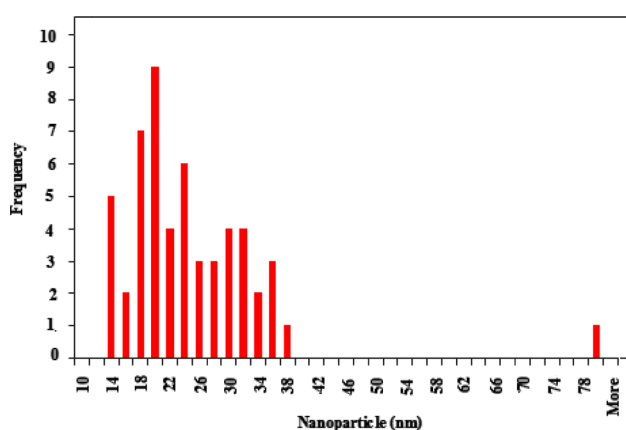


Fig. 5 Particle size distribution histogram of p(AMPS)-Ag (detection of particle average size of about 20 nm)

3.2 The catalytic activity of p(AMPS)-Ag toward the oxidation reaction of alcohols

The selective oxidation of alcohols, particularly with O_2 as the terminal oxidant, is one of the fundamental and important reactions in organic synthesis [19, 38]. With the p(AMPS)-Ag catalyst in hand, we aim to evaluate its catalytic activity for the aerobic oxidation of alcohols.

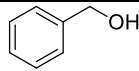
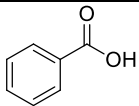
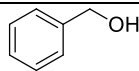
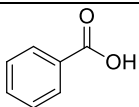
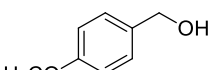
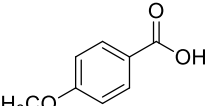
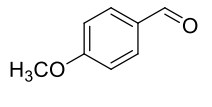
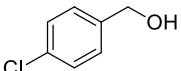
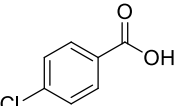
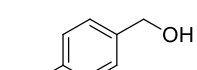
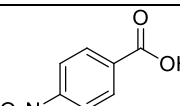
In the beginning, the oxidation reaction of the benzyl alcohol as the model substrate was done in water at 80 °C. The blank experiments without Ag loading exhibits a negligible benzyl alcohol conversion (<9% at 80 °C and 24 h reaction time). However, in the presence of the Ag catalyst, benzyl alcohol conversion increases. Within 24 h and with 0.05 g catalyst (0.22 mmol Ag), 38.5% isolated yield of the

benzoic acid was acquired. Within 24 h and with 0.1 g catalyst (0.44 mmol Ag), 65% isolated yield of the benzaldehyde was obtained (Table 2, entries 1–2).

Encouraged by these promising results, we then directed our attention toward the oxidation of other primary benzyl alcohols with substituent such as 4-MeO, 4- NO_2 and 4-Cl groups (Table 2, entries 3–5). All substrates were oxidized to the corresponding benzoic acid in good yields and excellent selectivity. The substitution effect on aromatic substrates was studied. As shown in Table 2, the conversion of alcohols, increased in the presence of electron-donating substituent, such as -OMe at the *para*- position of benzyl alcohol, (Table 2, entry 3), but in contrast, withdrawing group, such as NO_2 and Cl (Table 2, entries 4–5) decreased the conversion [39]. This trend is in accord with *Hammett* plot results and suggesting that the formation of the transition state with a carbocationic character on the benzylic carbon during the discharge of hydrogen in the rate-determining step is involved in the oxidation pathway over the current catalysts [40].

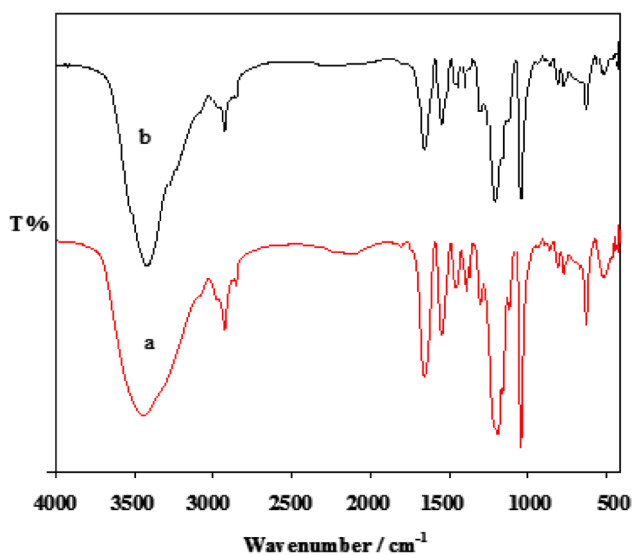
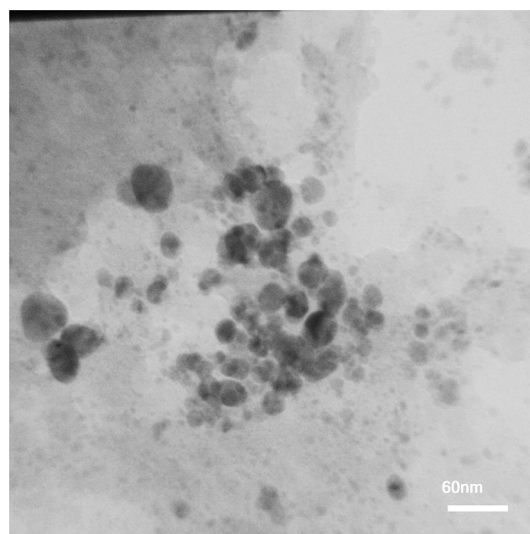
After reaction, the catalyst recovered by filtration was washed with H_2O , dried and reused for the next run without adding any fresh catalyst. The catalytic reusability for p(AMPS)-Ag in oxidations of benzyl alcohol was measured by four-run tests in H_2O solvent. The catalytic activity of catalyst is preserved even after 4 runs and yield of the reaction does not change significantly. Atomic adsorption spectroscopy of reaction mixture after catalyst separation also confirmed that no free silver ions are present in the solution. The stability of the supported catalyst was also investigated. In these experiments, the catalyst was separated from the reaction mixture after each experiment, washed, dried and characterized by FT-IR and

Table 2 Catalytic activity of p(AMPS)-Ag on the oxidation of benzyl alcohol

Entry	Substrate	Catalyst amount g catalyst (mmol Ag)	Conversion ^a (%)	Product	Selectivity (%)
1		0.05 g (0.22 mmol)	38.5		>99
2		0.1 g (0.44 mmol)	65		>99
3		0.1 g (0.44 mmol)	80		50
					50
4		0.1 g (0.44 mmol)	42		>99
5		0.1 g (0.44 mmol)	27		>99

Catalyst (0.1 g, 0.44 mmol Ag), substrate (1.0 mmol), H₂O, (5 mL) as solvent, K₂CO₃ 1.2 mmol, temperature 80 °C, Time=24 h under O₂ atmosphere

^aConversions are based on the starting substrate

**Fig. 6** FT-IR spectra of (a) fresh catalyst, (b) recycled catalyst**Fig. 7** TEM image of recycled p(AMPS)-Ag composite

TEM, as shown in Figs. 6, 7. FT-IR spectrum for the recovered p(AMPS)-Ag in Figs. 6 and 7 was well consistent with that of the fresh one, demonstrating a durable catalyst structure accounting for the steadily catalytic reuse.

3.3 The catalytic activity of p(AMPS)-Ag toward the reduction reaction of 4-nitrophenol

A reduction reaction relating the conversion of 4-NP to 4-AP was chosen as a model reaction to evaluate the catalytic activity of synthesized p(AMPS)-Ag composite. For this purpose, NaBH_4 was added as a reducing agent and p(AMPS)-Ag hydrogel composite as a catalyst. It should be noted that conversion of 4-NP to 4-AP cannot be carried out by NaBH_4 without assist of any catalyst [41]. According to thermodynamic studies, the reduction of nitro compounds is possible in the presence of excess amounts of aqueous solution of NaBH_4 , as reducing agent, with large kinetic barrier [42]. But, the attendance of a catalyst helps to overcome this energy barrier and makes these reactions feasible under mild conditions such as room temperature. In all the catalytic reduction of nitro aromatic compounds 0.02 g of hydrogel-Ag composite containing 0.088 mmol of Ag was used as catalyst.

Reduction of nitro compound was tracked by measuring the decrease in its absorbance peak in UV-Vis spectra taken at various intervals of times. Only a small amount of 4-NP was reduced in the absence of catalyst even after 3 h as shown in Fig. 8a. But after the addition of catalyst almost all of the 4-NP present in the reaction mixture was reduced within 70 min as demonstrated in Fig. 8b.

As reduction of NP was carried out in large excess of NaBH_4 so this reaction was supposed as pseudo first order and values of k_{app} were calculated by plotting $\ln(C_t/C_0)$ versus time as shown in Fig. 9. In order to evaluate the effect of temperature on the catalytic activity of p(AMPS)-Ag composite the reduction of 4-NP was investigated at three different temperatures; 25 °C, 40 °C, 60 °C keeping the amount of reactant and catalyst constant. Dependence of reaction rate on temperature is displayed in Fig. 9, ($\ln(C_t/C_0)$ versus time at different temperatures). The reduction rates were increased linearly as temperature rise. Because at higher temperature, rate of diffusion of reactant molecules into hydrogel composites and collision frequency of reactant and catalyst increase due to enhance in the average kinetic energy of molecules.

Activation parameters can be calculated from the data obtained by the reduction reactions carried out at different temperatures catalyzed by p(AMPS)-Ag composite. Energy of activation (E_a) was calculated from Arrhenius equation which is given below

$$\ln k = \ln A - (E_a/RT) \quad (1)$$

According the Arrhenius equation $\ln k_{app}$ was plotted against $1/T$ as shown in Fig. 10a, E_a was calculated from the

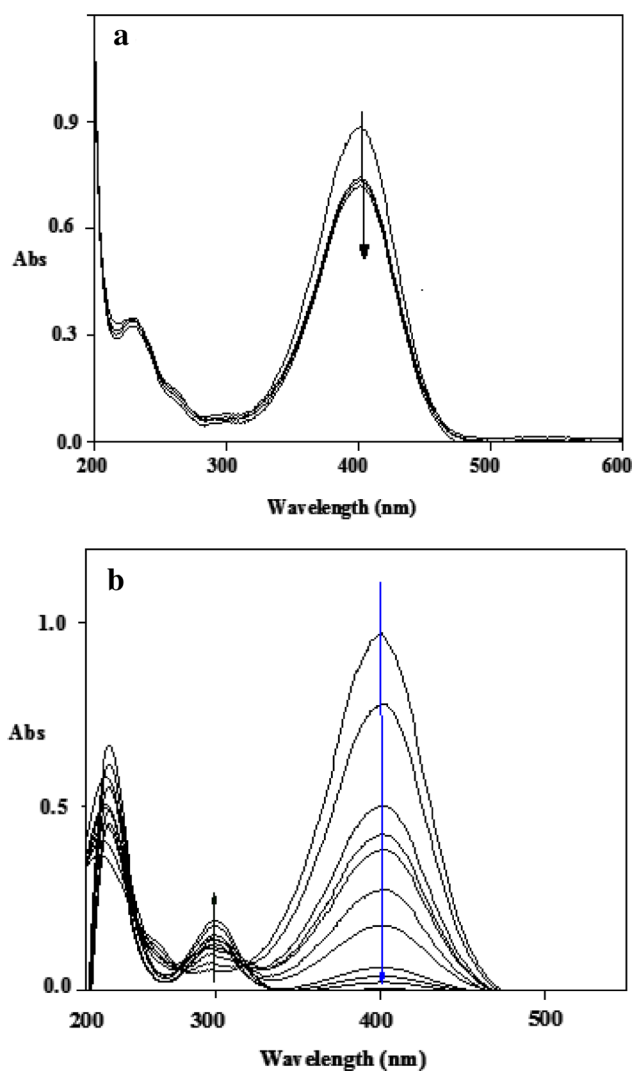


Fig. 8 **a** UV-Vis spectra of 4-NP in the absence of catalyst and presence of NaBH_4 . **b** UV-Vis spectra for the reduction of 4-NP catalyzed by p(AMPS)-Ag composite and NaBH_4 . Reaction conditions; 0.01 M 4-NP 50 mL, $\text{NaBH}_4=0.2$ M, 0.02 g catalyst equal to 0.088 mmol Ag, 25 °C

slope of this plot and found to be equal to $35.267 (\pm 0.375)$ kJ mol^{-1} .

The activation enthalpy (ΔH^\ddagger) and entropy (ΔS^\ddagger) were calculated by using Eyring equations (Eq. (2)).

$$\ln k/T = \ln (k_B/h) + \Delta S^\ddagger/R - \Delta H^\ddagger/R(1/T) \quad (2)$$

According to Eyring equation $\ln k_{app}/T$ was plotted against $1/T$ as shown in Fig. 10b. The value of ΔH^\ddagger was calculated from the slope of this plot and was found to be $32.649 (\pm 0.375)$ kJ mol^{-1} . The positive value of ΔH^\ddagger shows that the formation of an activated complex in the reduction of 4-NP is an endothermic process [43]. The value of ΔS^\ddagger was calculated from the intercept of plot of $\ln(k_{app}/T)$ versus $1/T$ and was found as $-158.875 (\pm 0.889)$ $\text{J mol}^{-1} \text{K}^{-1}$. The

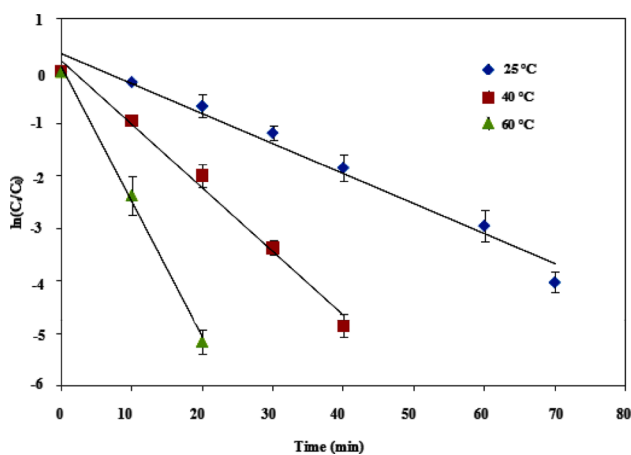


Fig. 9 The determination of apparent rate constants (k_{app}) for the reduction 4-NP catalyzed by p(AMPS)–Ag composites with temperature

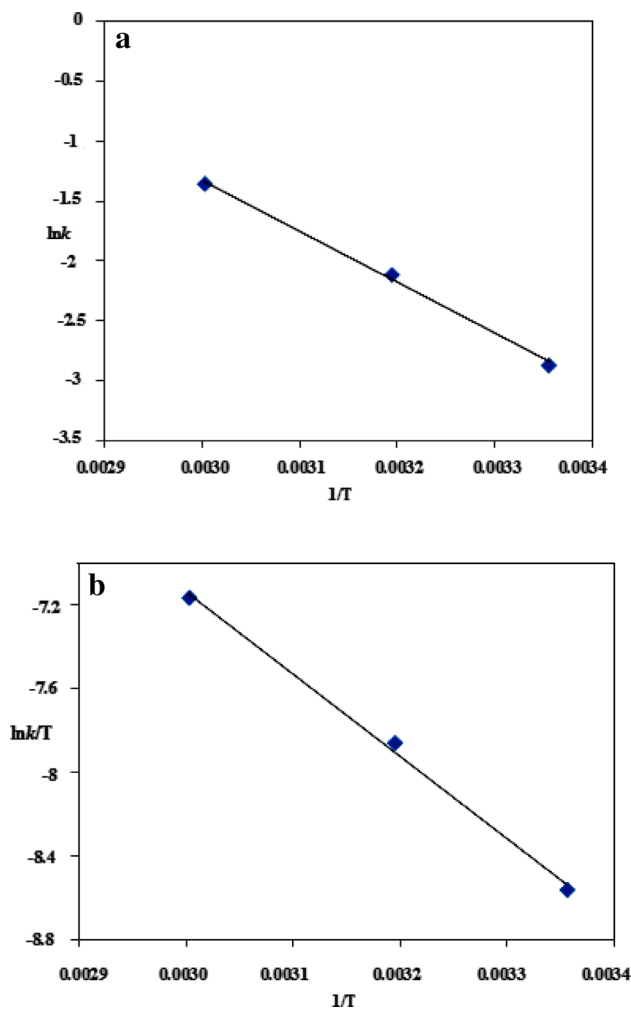


Fig. 10 The determination of apparent rate constants (k_{app}) for the reduction 4-NP catalyzed by p(AMPS)–Ag with temperature, **a** plot of $\ln(k_{app})$ versus $1/T$, **b** Plot of $\ln(k_{app}/T)$ versus $1/T$ for the reduction 4-NP catalyzed by p(AMPS)–Ag with temperature

negative value of ΔS^\ddagger shows that the reduction of 4-NP is entropically unfavorable which can be made favorable by adding catalyst [43]. The value of ΔG^\ddagger was calculated from the following equation, $\Delta G^\ddagger = \Delta H^\ddagger - T\Delta S^\ddagger$

The values of ΔG^\ddagger at 298 K, 313 K and 333 K were calculated as 79.994 kJ mol⁻¹, 83.377 kJ mol⁻¹, 85.554 kJ mol⁻¹, respectively. The positive values of ΔG^\ddagger shows that reduction of 4-NP is a non-spontaneous process [44] and it needs an input energy to proceed which is provided by the addition of the catalyst.

The effect of catalyst amount on the reduction rate of 4-NP was also investigated. The reaction was studied at three different amounts of catalyst viz. 0.01, 0.02, 0.04 g. As shown in Fig. 11a, with an increase in catalyst amount, the increase in rate of reaction was observed, as expected. As with the increase in amount of catalysts, the available catalytic sites are also increased. According to availability of greater number of catalytic sites, greater numbers of reactants are adsorbed on the surface of catalyst at the same time, which results in an increase in rate of formation of the products.

In order to investigate the effect of amount of reducing agent on the reduction rate, different amounts of NaBH₄

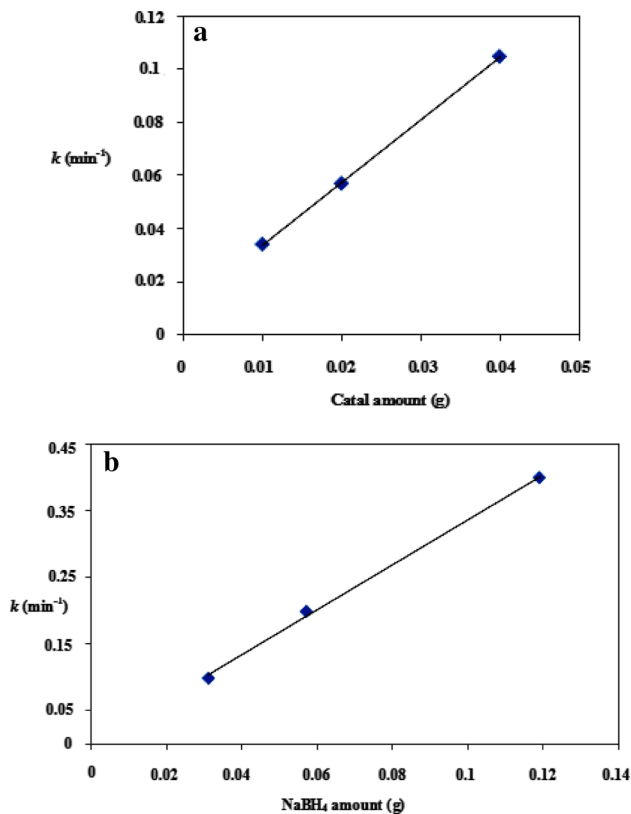


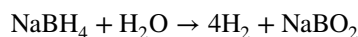
Fig. 11 a The change in reduction rate constant of 4-NP with the amount of Ag catalyst inside p(AMPS)–Ag composites; **b** Change in values of k_{app} with the change in of concentration of NaBH₄ during the reduction of NP

were used by assuming all other parameters constant. For evaluation the effect of NaBH_4 on the reduction rate, different amounts of NaBH_4 (0.1–0.4 M) were used in reduction of 4-NP. As can be seen from Fig. 8b, there is a linear increase in the reduction rate of 4-NP with the increase in the amount of NaBH_4 at 25 °C. The same trend has been reported in several literatures [45].

The reusability of p(AMPS)–Ag catalyst system was studied by using the same catalyst in 4-NP reduction repeatedly up to four times. After every use, the catalyst was filtered and washed with DI, and used again for the same reaction under the same reaction conditions without significant loss of activity.

3.4 H_2 production by hydrolysis of NaBH_4

Finally, metal nanoparticle containing hydrogel composites was used in hydrogen generation reactions from hydrolysis of NaBH_4 under stable reaction conditions of 50 mL 0.1 M NaBH_4 , at 25 °C. Each hydrolysis reaction in this study was repeated at least three times and the average of these measurements was calculated with standard deviation.



The H_2 generation reactions from hydrolysis of NaBH_4 were performed at three different temperatures to understand the effect of temperature and calculate the activation parameters. It was found that temperature is highly effective on H_2 generation reactions from hydrolysis of NaBH_4 . The effect of the temperature on the hydrolysis of NaBH_4 was determined by using 0.1 g p(AMPS)–Ag metal composites (containing 0.44 mmol nanoparticles) at different temperatures which changed between 25 and 60 °C under certain reaction conditions as given in experimental section. As the temperature of the reaction medium is increased, the times to produce the same amount of H_2 was decreased as demonstrated in Fig. 12a. As can be seen the H_2 generation reaction was completed within about 110 min at 25 °C whereas the same reaction was completed within about 30 min at 60 °C. The thermodynamic parameters of the hydrolysis reaction of NaBH_4 were calculated by using the very well known Arrhenius (Eq. (1)) and Eyring (Eq. (2)) equations associated with the graphs $\ln k$ versus $1/T$ and $\ln(k/T)$ versus $1/T$ graphs as given in Fig. 12b, c, respectively.

As can be seen from Fig. 10, $\ln k$ versus $1/T$ and $\ln(k/T)$ versus $1/T$ provide good linear relation. However, the activation energy was calculated by applying Eq. (1) for different temperature, the same data were also used by applying Eq. (2) for in calculation of activation enthalpy and entropy. The activation parameters of energy, enthalpy and entropy of p(AMPS)–Ag metal composite systems were determined as $E_a = 29.95 \text{ kJ mol}^{-1}$, $\Delta H^\ddagger = 27.33 \text{ kJ mol}^{-1}$ and $\Delta S^\ddagger = -94.23 \text{ J mol}^{-1} \text{ K}^{-1}$, respectively (Fig. 13).

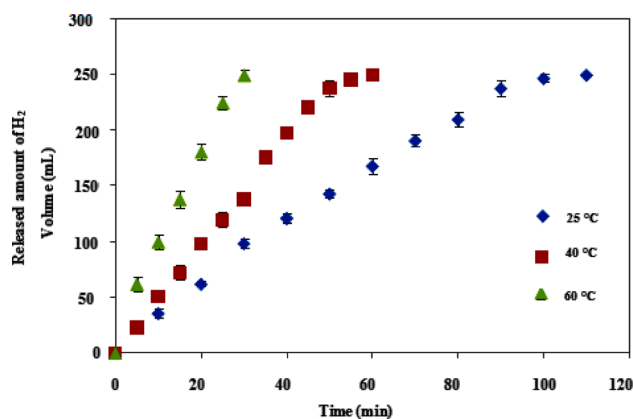


Fig. 12 The effects of temperature on the hydrolysis of NaBH_4 , (b) $\ln k$ versus $1/T$ (Arrhenius eq. and (c) $\ln(k/T)$ versus $1/T$ (Eyring eq.). [50 mL 50 mM NaBH_4 , 0.44 mmol Ag in 0.1 g p(AMPS)–Ag hydrogel-metal composite]

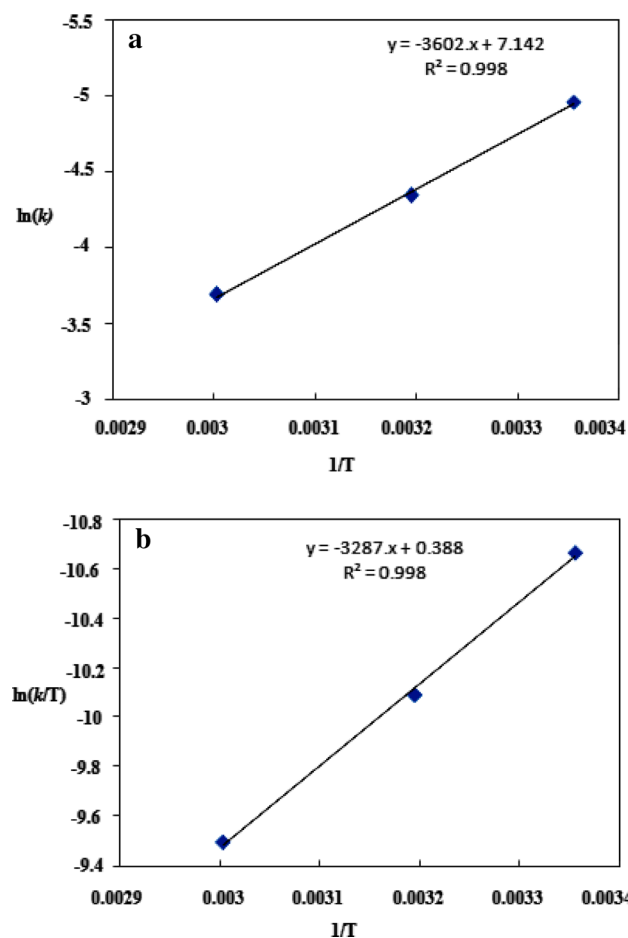


Fig. 13 a $\ln k$ versus $1/T$ (Arrhenius eq.) b, and $\ln(k/T)$ versus $1/T$ (Eyring eq.)

4 Conclusion

Synthesis of p(AMPS) hydrogel was accomplished by a very simple and easy method of free radical polymerization and Ag nanoparticles were prepared within the hydrogel network by in situ reduction method. FT-IR spectroscopy, AA measurement and TEM images demonstrated the existence of silver nanoparticles in p(AMPS) hydrogel matrix. The prepared composites were found to be very effective catalysts toward oxidation reaction of benzyl alcohols, reduction of 4-nitrophenol and hydrogen generation from the hydrolysis of NaBH_4 under green conditions such as easy separation of the catalyst, using water as solvent and relatively low temperature. Reuse of the catalysts can be achieved, without significant loss of catalytic activity.

Acknowledgements Authors are thankful to University of Zanjan for financial support of this study.

References

- F. Naseer, M. Ajmal, F. Bibi, Z.H. Farooqi, M. Siddiq, *Polym. Compos.* **39**, 3187 (2018)
- N. Sahiner, H. Ozaya, O. Ozay, N. Aktas, *Appl. Catal. A* **385**, 201 (2010)
- B.A. Cheney, J.A. Lauterbach, J.G. Chen, *Appl. Catal. A* **394**, 41 (2011)
- N. Zheng, G.D. Stucky, *J. Am. Chem. Soc.* **128**, 14278 (2006)
- M. Boualleg, J.M. Basset, J.P. Candy, P. Delichere, K. Pelzer, L. Veyre, C. Thieuleux, *Chem. Mater.* **21**, 775 (2009)
- D. Liu, J. Gao, C.J. Murphy, C.T. Williams, *J. Phys. Chem. B* **108**, 12911 (2004)
- A. Singh, B.D. Chandler, *Langmuir* **21**, 10776 (2005)
- M.A. Albiter, F. Zaera, *Langmuir* **26**, 16204 (2010)
- H. Ozay, S. Kubilay, N. Aktas, N. Sahiner, *Int. J. Polym. Mater.* **60**, 163 (2011)
- N. Sahiner, H. Ozay, O. Ozay, N. Aktas, *Appl. Catal. B* **101**, 137 (2010)
- O. Ozay, N. Aktas, E. Inger, N. Sahiner, *Int. J. Hydrog. Energy* **36**, 1998 (2011)
- N. Sahiner, S. Butun, O. Ozay, B. Dibek, *J. Colloid Interface Sci.* **373**, 122 (2012)
- M. Zhong, Y.T. Liu, X.M. Xie, *J. Mater. Chem. B* **3**, 4001 (2015)
- Y. Wang, R. Yan, J. Zhang, W. Zhang, *J. Mol. Catal. A* **317**, 81 (2010)
- D.G. Lee, U.A. Spitzer, *J. Org. Chem.* **35**, 3589 (1970)
- H. Tsunoyama, H. Sakurai, Y. Negishi, T. Tsukuda, *J. Am. Chem. Soc.* **127**, 9374 (2005)
- Y.M.A. Yamada, T. Arakawa, H. Hocke, Y. Uozumi, *Angew. Chem. Int. Ed.* **46**, 704 (2007)
- S. Kanaoka, N. Yagi, Y. Fukuyama, S. Aoshima, H. Tsunoyama, T. Tsukuda, H. Sakurai, *J. Am. Chem. Soc.* **129**, 12060 (2007)
- M. Ghorbanloo, A. Heydari, H. Yahiro, *Appl. Organomet. Chem.* **32**, e3917 (2018)
- A. Abad, A. Corma, H. Garcia, *Chem. Eur. J.* **14**, 212 (2008)
- P. Haider, J.D. Grunwaldt, R. Seidel, A. Baiker, *J. Catal.* **250**, 313 (2007)
- J. Chen, Q. Zhang, Y. Wang, H. Wan, *Adv. Synth. Catal.* **350**, 453 (2008)
- M. Ghorbanloo, N. Moharramkhani, T. Mokary Yazdely, H.H. Monfard, *J. Porous Mater.* **26**, 433 (2019)
- A. Biffis, L. Minati, *J. Catal.* **236**, 405 (2005)
- Z. Opre, J.D. Grunwaldt, M. Maciejewski, D. Ferri, T. Mallat, A. Baiker, *J. Catal.* **230**, 406 (2005)
- L. Ai, X. Gao, J. Jiang, *J. Power Sources* **257**, 231 (2014)
- S. Zinoviev, F. Muller-Langer, P. Das, N. Bertero, P. Fornasiero, M. Kaltschmitt, G. Centi, S. Miertus, *ChemSusChem* **3**, 1106 (2010)
- M. Li, D.A. Cullen, K. Sasaki, N.S. Marinkovic, K. More, R.R. Adzic, *J. Am. Chem. Soc.* **135**, 132 (2013)
- J. Zhu, R. Li, W. Niu, Y. Wu, X. Gou, *Int. J. Hydrog. Energy* **38**, 10864 (2013)
- L. Ai, X. Gao, J. Jiang, *J. Power Sources* **257**, 213 (2014)
- R. Retnamma, A.Q. Novais, C.M. Rangel, *Int. J. Hydrog. Energy* **36**, 9772 (2011)
- U.B. Demirci, P. Miele, *Phys. Chem. Chem. Phys.* **12**, 14651 (2010)
- N. Sahiner, A. Kaynak, S. Butun, *J. Non-Cryst. Solid* **358**, 758 (2012)
- A.J. Chaudhary, S.M. Grimes, *Chemosphere* **72**, 1636 (2008)
- U.S. Environmental Protection Agency, *Nitrophenols, Ambient Water Quality Criteria* (U.S. Environmental Protection Agency, Washington, DC, 1980)
- L. Wangyang, C. Wenxing, L. Nan, X. Minhong, Y. Yuyuan, *Appl. Catal. B* **87**, 146 (2009)
- S. Demirci, N. Sahiner, *Water Air Soil Pollut.* **226**, 64 (2015)
- B. Karimi, S. Abedi, J.H. Clark, V. Budarin, *Angew. Chem. Int. Ed. Engl.* **45**, 4776 (2006)
- P.D. Sharma, P. Panchariya, P. Purohit, P.K. Sharma, *Eur. Chem. Bull.* **2**, 816 (2013)
- T. Harada, S. Ikeda, F. Hashimoto, T. Sakata, K. Ikeue, T. Torimoto, M. Matsumura, *Langmuir* **26**, 17720 (2010)
- M. Ghorbanloo, A. Heydari, H. Yahiro, *Desalin. Water Treat.* **115**, 106 (2018)
- M. Ajmal, M. Siddiq, M.H. Al-Lohedanc, N. Sahiner, *RSC Adv.* **4**, 59562 (2014)
- M. Ajmal, S. Demirci, M. Siddiq, N. Aktas, N. Sahiner, *Colloid. Surf. A* **486**, 29 (2015)
- Z.H. Farooqi, A. Ijaz, R. Begum, Z. Naseem, M. Usman, M. Ajmal, U. Saeed, *Polym. Compos.* **39**, 645 (2018)
- S. Butun, N. Sahiner, *Polymer* **52**, 4834 (2011)

Publisher's Note Springer Nature remains neutral with regard to jurisdictional claims in published maps and institutional affiliations.